

Towards R-Space Bose-Einstein Condensation of Photonic Crystal Exciton Polaritons

D. L. Boiko

Sowoon Technologies S.á.r.l., 1015, Lausanne, Switzerland

Abstract— Coupled states of semiconductor quantum well (QW) excitons and photons in a two dimensional (2D) periodic lattice of microcavities are analyzed theoretically, revealing allowed bands and forbidden gaps in the energy spectrum of exciton polaritons. Photonic crystal exciton polaritons have spatially uniform excitonic constituent set by flat QWs, but exhibit periodic Bloch oscillations in the plane of QWs due to their photonic component. The envelope functions of photonic crystal exciton polaritons can be tailored via effective potential of a photonic crystal heterostructure, by using quasi-periodic lattices of microcavities. Confined envelope function states of lower and upper polaritons and the Bose-Einstein condensation of lower polaritons are analyzed here in a photonic crystal heterostructure trap with harmonic oscillator potential. This concept is numerically illustrated on example of CdTe/CdMgTe microcavities.

1. INTRODUCTION

Recently, several claims have been made on achieving the Bose-Einstein condensation (BEC) in solids [1, 2, 3, 4]. In these experiments, semiconductor microcavities incorporating heterostructure quantum wells (QWs) sandwiched between two distributed Bragg reflectors (DBRs) are used in a strong-coupling regime, such that the coupled states of QW excitons and cavity photons represent composite (bosonic) quasiparticles. Due to photonic constituent, the cavity exciton polaritons are of light effective masses (10^{-4} of free electron mass) and allow the macroscopic quantum degeneracy to be achieved at lower density and higher temperature compared to the BEC transition in an atomic vapor. Nevertheless, the recent reports on k-space BEC and early observations of macroscopic coherence in polariton system (*e.g.*, Refs.[5, 6]) allow one to argue that these observations may not be attributed uniquely to the BEC phase transition (*e.g.*, Ref.[7]).

Incompleteness of experimental data and a short lifetime of the cavity exciton polaritons do not allow a thermalization and spontaneous transition to a macroscopically ordered state to be unambiguously confirmed. Thus in [1, 3, 4], a correlation function of the first order $g^{(1)}$ is measured to prove the fact of macroscopic quantum coherence. However, such phase correlations may not be attributed uniquely to a quantum coherent state, which assumes that $g^{(n)} \equiv 1$ for any order n [8]. In particular, the first order correlations can also be observed in a chaotic thermal state [9, 10, 11]. Therefore, other tests verifying the nature of a macroscopically ordered state of exciton polaritons are important.

A harmonic oscillator trap with confining potential $U = \frac{1}{2}\alpha_{LP}r^2$ for lower polaritons (LPs) can provide an evidence of BEC by displaying distinct spatial distributions of polaritons in the condensate and non-condensate fractions [12]. In [4], a claim is made on achieving r-space BEC of GaAs cavity exciton polaritons in a trap produced via excitonic component of polaritons, by introducing the Pikus-Bir deformation potential $U = \frac{1}{2}\alpha_X r^2$ for excitons (X) in GaAs QWs. The reported force constant of the trap for lower polaritons $\alpha_{LP} = 480 \text{ eV/cm}^2$ assumes that the corresponding trapping potential for excitons is of $\alpha_X = 1150 \text{ eV/cm}^2$, which improves by a factor of 30 the force constant of a trap previously reported for GaAs QW excitons [13]. However, the features of the coherent fraction of LPs, which was delocalized over a region of $8 \mu\text{m}$ size, were different from the expected point-like localization of r-space BEC condensate fraction. This discrepancy might be attributed to a negative photon-exciton energy detuning inherent to stress-induced traps, since such negative energy detuning prevents thermalization of lower polaritons [2]. These allow one to question whether the reported observations indeed might be attributed to the r-space BEC of cavity exciton polaritons and whether such traps with negative photon-exciton relative energy are suitable for BEC experiments.

In this paper, a novel concept of harmonic oscillator trap for exciton polaritons is proposed, benefiting from the light propagation features in quasi-periodic 2D arrays of optically coupled

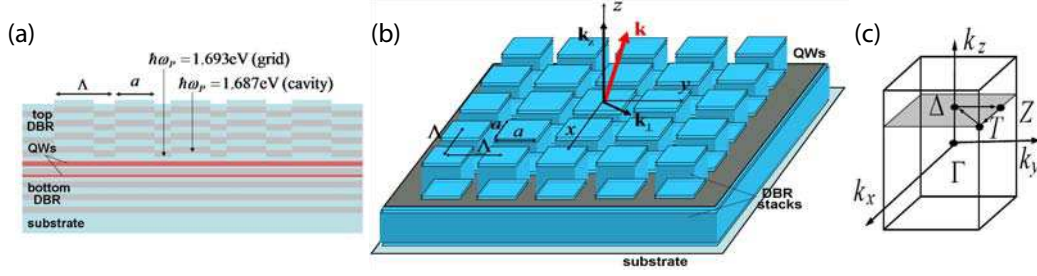


Figure 1: Photonic crystal harmonic oscillator trap implemented with quasi-periodic 2D array of coupled microcavities. (a): Schematic of the wafer structure with etched array of shallow mesa pixels at the cavity spacer layer and regrown top DBR structure. (b): Schematic of the array with parabolically varying size of microcavity pixels used to define effective potential for exciton polaritons. (c): Brillouin zone of a square lattice array of microcavities. Λ is the lattice pitch, a is the width of the cavity pixels.

microcavities. Such photonic crystal lattices oriented in the plane of QWs are shown here to induce periodic Bloch oscillations in exciton polariton wave functions. By introducing tailored variations of the cavity pixels across an array, an effective potential can be superimposed on these oscillations to control the envelop wave functions of photonic crystal exciton polaritons. This opens the way to trap polaritons in a harmonic oscillator potential at a positive photon-exciton detuning, by shaping the photonic constituent of polaritons. Such traps will favor thermalization of lower polaritons in experiments on r-space BEC. This concept is numerically illustrated here on example of harmonic oscillator trap implemented with array of CdTe/CdMgTe microcavities.

The paper is organized as follows. Sec. 2 details a structure of arrays of coupled microcavities treated here. In Sec. 3, the photonic crystal exciton polaritons are analyzed in a uniform-lattice arrays. In Sec. 4, a photonic crystal heterostructure trap for exciton polariton is considered. The properties of non-condensate and condensate fractions of lower polaritons in the trap are discussed in Sec. 5.

2. QUASI-PERIODIC ARRAY OF COUPLED MICROCAVITIES

The microcavities discussed here are arranged in a quasi-periodic two dimensional lattice (Fig. 1). Such arrays of optically coupled microcavities belong to a particular class of paraxial photonic crystal (PhC) structures, in which the light propagates mostly normal to the periodic lattice plane [14, 15]. These structures employ lattices of periods significantly exceeding the optical wavelength. For example, the arrays of CdTe/CdMgTe microcavities treated here employ lattices of $3 \mu\text{m}$ pitch (Fig. 1) and have a vertical cavity structure (one-wavelength cavity incorporating QWs and sandwiched between two DBRs) optimized at 730 nm wavelength. In such structures, only a small transversal component of wave vector \mathbf{k} of a photon undergoes periodic Bragg reflections in the optical lattice plane. The main \mathbf{k} -vector component (along the cavity z -axis in Fig. 1) is fixed by the cavity roundtrip self-repetition condition.

These arrays can be fabricated by introducing intermediate processing steps during a wafer growth (*e.g.*, shallow mesa-etching) such that microcavities share multiple QWs in the λ -cavity and in the few first periods of the bottom DBR. In this way, a periodic photonic crystal lattice can be defined in the plane of QWs, as indicated in Fig. 1. By analogy with the cavity exciton polaritons in broad-area microcavities, the coupled states of QW excitons and photons in coupled arrays of microcavities are termed here as photonic crystal exciton polaritons. (As shown in Sec. 3, their wave functions exhibit periodic Bloch oscillations in the plane of QWs.) As in the solitary microcavities utilizes in experiments on k-space BEC [1, 2, 3, 4], there are two degrees of freedom available for photonic crystal exciton polaritons to form spontaneously a microscopically ordered state.

Lattices of CdTe/CdMgTe microcavities analyzed here theoretically are defined by etching a periodic pattern of shallow mesa structures at the cavity spacer layer and subsequently regrowing a complete top DBR structure (Fig.1). This periodic pattern is used to define the position of cavity pixels. In the model calculations, a vertical composition of the cavity wafer is similar to the one of Ref.[1]. In particular, the cavities incorporating 16 quantum wells with exciton energy of 1.682 eV and Rabi energy splitting of 26 meV are analyzed. The vertical-cavity modes oscillate at photon energies of 1.687 and 1.693 eV at the cavity pixels and array grid separating the pixels, respectively.

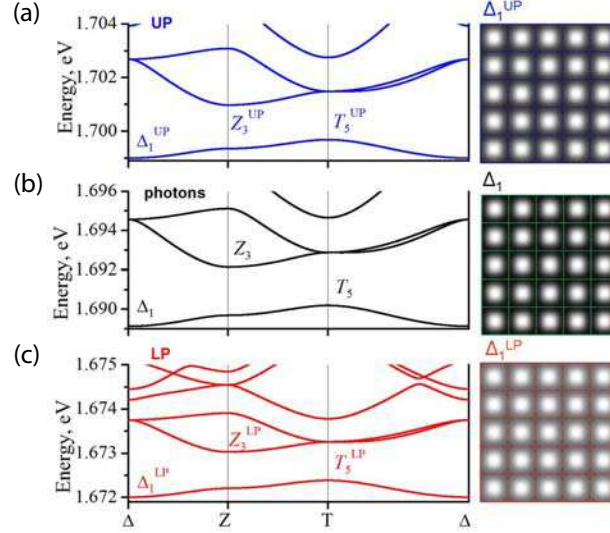


Figure 2: Energy bands (left panels) and lowest-energy state wave functions $|\psi(x, y)|^2$ (right panels) of the upper polaritons (a), photons (b) and lower polaritons (c) in a periodic lattice of coupled CdTe/CdMgTe microcavities ($FF = 0.5$, $\Lambda = 3 \mu\text{m}$). The panels (a)-(c) are ordered according the energy scale.

Such tiny variations in the resonant energy of vertical-cavity modes ($\sim 0.3\%$) suffice to define a lattice of paraxial photonic crystal [14]. As shown below, low-contrast lattices considered here allow a forbidden energy gap to be opened in the spectrum of coupled optical modes of entire array structure. Another important parameter, which impacts the photonic band structure, is the lattice cell fill factor (FF) defined as the area ratio of the cavity pixel and of the lattice cell. For square arrays treated here, the lattice period Λ is $3 \mu\text{m}$ and the lattice cell fill factor FF varies in the range of $0.5-1$ ($FF = a^2/\Lambda^2$, with a being the square pixel width).

3. PHOTONIC CRYSTAL EXCITON POLARITON

Fig. 2 (b) shows optical mode dispersion curves for a uniform array of microcavities with the lattice fill factor of $FF=0.5$ ($2.1 \mu\text{m}$ cavity pixels arranged in a square lattice of $3 \mu\text{m}$ pitch). The photonic band structure was calculated using the paraxial Hamiltonian approach developed in Refs. [14, 15]. The energy bands are plotted along the high symmetry lines of the Brillouin zone [Fig. 1(c)]. The wave vector \mathbf{k} of a photon is $(0, 0, k_z)$, $(0, \pi/\Lambda, k_z)$ and $(\pi/\Lambda, \pi/\Lambda, k_z)$ at the Δ , Z and T points of the Brillouin zone (BZ), respectively.

It can be seen that for low-contrast structures considered here, a complete 2D band gap is opened between the states in the T and Z points of the BZ [14, 15]. In Fig. 2 (b), the forbidden energy gap is of 2 meV. Note that the optical modes originating from equivalent T points of the BZ show a π phase shift between adjacent lattice sites (the out-of-phase modes) while the modes located at the Z points of the BZ exhibit the out-of-phase oscillations along only one lattice direction and they oscillate in-phase at the lattice sites located along the second direction of the lattice [14, 15].

Within the framework of this study centered on photonic crystal exciton polaritons, the most important photonic state is the lowest energy state Δ_1 located at the Δ point of the BZ. In this state, the optical mode shows no phase shift at adjacent lattice sites, such that oscillations of the electromagnetic field are in-phase at all microcavities composing the lattice. The intensity distribution of the Δ_1 optical mode reveals periodic Bloch oscillations in the plane of QWs [Fig. 2(b), right panel]. As expected by the lattice fill factor considerations ($FF=0.5$), this mode oscillates at intermediate photon energy of 1.691 eV compared to the vertical-cavity modes at the array pixel (1.687 eV at $FF=1$) and at the grid (1.693 eV at $FF=0$). Correspondingly, the energy of the ground state Δ_1 can be modified within this range by varying the lattice cell fill factor FF . It can be then seen that a positive energy difference between a photon in the Δ_1 state and QW exciton is maintained at any FF of the lattice. [In Fig. 2, the QW exciton of 1.682 eV energy is located in between the energy scales shown in panels (b) and (c).]

The coupled states of PhC photons and QW excitons are analyzed here using Jaynes-Cummings model that takes into account the coupling between a QW exciton and vacuum field oscillations in a PhC mode. The top and bottom panels in Fig. 2 show, respectively, the upper polariton (UP)

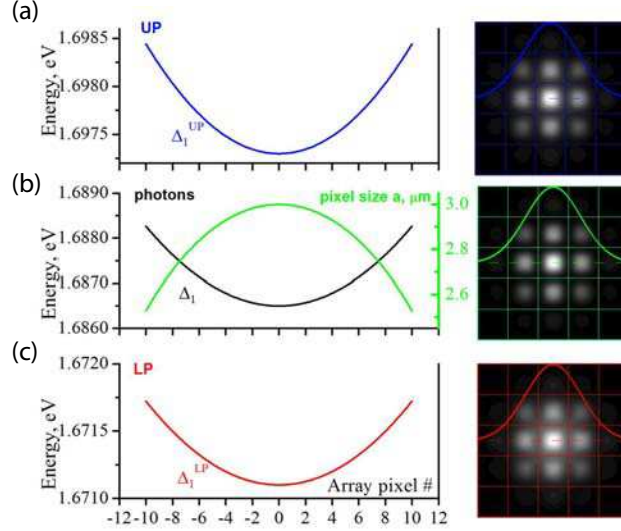


Figure 3: Parabolically graded band edges of lowest-energy bands (left panels) and ground-state probability densities $|\psi(x, y)|^2$ (right panels) of the upper polaritons (a), photons (b) and lower polaritons (c) in the trap defined by tailored pixel-size variations [green curve in (b), right axis] in a quasi-periodic 2D array of coupled CdTe/CdMgTe microcavities ($\Lambda = 3 \mu\text{m}$). The panels (a)-(c) are ordered according to the energy scale.

and lower polariton (LP) energy bands as well as the coordinate probability distribution functions $|\psi(x, y)|^2$ for the upper and lower polariton states of lowest energies (the states Δ_1^{UP} and Δ_1^{LP}), calculated using the Rabi coupling constant $2\Omega_R = 26 \text{ meV}$.

It can be seen that due to a photonic constituent, the features of periodic Bragg reflections in the plane of photonic crystal lattice are transferred to exciton polaritons. Thus, the energy dispersion curves of UP and LP (Figs. 2 (a) and (c), left panels) show energy bands separated by forbidden gaps. Respectively, the wave functions of exciton polaritons exhibit periodic Bloch oscillations. In the case of uniform photonic lattices, these periodic oscillations are modulated with plane wave envelope functions propagating in the plane of QWs.

As indicated by the modulation contrast of the $|\psi(x, y)|^2$ distributions, due to contribution of excitons from flat QWs, the Bloch oscillations are less pronounced in the UP and LP wave functions as compared to photons. Furthermore, in Fig. 2, the lower polariton states have higher excitonic content and they are characterized by smoother energy bands and wave function distributions, as compared to the upper polaritons. Nevertheless, the features of periodic Bloch oscillations are clearly visible in the LP wave functions and one can expect that the envelope functions of polaritons can be tailored by using photonic crystal heterostructures.

4. HARMONIC OSCILLATOR TRAP FOR EXCITON POLARITONS

Trapping of exciton polaritons in a harmonic oscillator potential is accomplished here via their envelope wave functions. A photonic crystal heterostructure trap is defined by introducing tailored variations of the cavity pixel size across the array structure.

A numerical analysis shows that for the low-contrast lattices considered here and for the lattice cell fill factor FF in the range of 0.1–1, the Δ_1 photonic band edge energy decreases monotonically with increasing cavity pixel size a . Therefore, the pixel-size variations $\propto -(x^2 + y^2)$ along the two lattice directions of an array produce a parabolically graded shift ($\propto r^2$) of the photonic band edge Δ_1 . Fig. 3 (b) shows variations of the pixel size with the lattice position (right axis, green curve) and the resulting effective potential profile $U_P = \frac{1}{2}\alpha_P r^2$ for photons (left axis, black curve).

When an exciton from a flat QW forms a coupled state with a photon in the effective potential U_P , the upper (Δ_1^{UP}) and lower (Δ_1^{LP}) polariton bands exhibit parabolic variations of the band edge with the lattice position as well. These variations define the effective confining potentials $U_{UP} = \frac{1}{2}\alpha_{UP} r^2$ and $U_{LP} = \frac{1}{2}\alpha_{LP} r^2$ for the upper and lower polaritons (Fig. 3(a) and (c), respectively). In Fig. 3, the effective force constants of the trap are $\alpha_P = 390$, $\alpha_{UP} = 250$ and $\alpha_{LP} = 140 \text{ eV}/\text{cm}^2$ for the photons, UP and LP states, respectively.

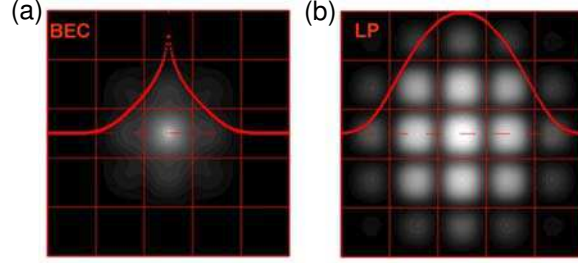


Figure 4: Probability density distributions and envelope function cross-sections for the LPs in the BEC fraction (a) and in the ground oscillator state (b) plotted across a region of 5×5 lattice sites of a quasi-periodic array of CdTe/CdMgTe microcavities (the array pitch is $\Lambda = 3 \mu m$). In both cases, a logarithmic scale $\propto M \ln(1 + |\psi(x, y)|^2/p_{th})$ is used with the probability density threshold of $p_{th} = 10^{-3}$, but different scale factors M are applied to the macroscopic wave function (a) and single-polariton wave function (b).

The confined envelope functions of exciton polaritons in the trap are analyzed here using the effective mass approximation [15] with effective masses derived from the energy dispersion curves in the vicinity of the Δ point of the BZ. The effective masses of a photon (in the plane of QWs), UP and LP are, respectively, $m_P = 0.9 \cdot 10^{-4} m_e$, $m_{UP} = 1.4 \cdot 10^{-4} m_e$ and $m_{LP} = 2.4 \cdot 10^{-4} m_e$, with m_e being the free electron mass. The larger mass of lower polariton is due to the higher excitonic content in LP states, in agreement with the features of periodic Bloch oscillations in probability density $|\psi(x, y)|^2$ (Fig. 2).

The calculated trap force constants and effective masses assume that the excitation energies $\hbar\omega_{osc} = \sqrt{\alpha/m^*}$ of photonic, UP and LP oscillators are of 59, 38 and 21 μeV , respectively. These energies also define a shift of corresponding ground oscillator states from the bottom of the trap.

The wave functions of photons, UPs and LPs in the ground state of the trap are indicated in Figs.3(a)-(c) (right panels). They exhibit periodic Bloch oscillations modulated with the Gaussian envelope functions delocalized over several lattice sites. The envelope functions for the photons, UPs and LPs are almost identical to each other. The apparent difference between the spatial distributions of probability densities in Fig. 3 is caused by dissimilar Bloch functions of photons and polaritons.

5. RESULTS AND DISCUSSION

In previous sections, the interactions in the LP system have not yet been taken into account and the analysis of confined states in the trap has been carried out in the effective mass approximation, using stationary Schrödinger equation. Introducing a term $\propto |\psi(x, y)|^2$, which accounts for small repulsive interactions in the polariton system, one obtains a nonlinear Gross-Pitaevskii equation for lower polaritons. Its solution at zero chemical potential represents a condensate fraction of LPs. In Fig.3(c), this state is located at the bottom of the trap, at 21 μeV below the ground oscillator state.

The macroscopic wave function of the lower polariton condensate is shown in Fig. 4(a) (logarithmic scale). The condensate fraction is localized to a single cavity pixel at the center of the trap. The excitonic content of lower polaritons in this state is of 0.6. For comparison, Fig. 4(b) shows the LP wave function in the ground oscillator state, plotted in the logarithmic scale as well. The spatial distribution of polaritons in the condensate fraction (a) is thus significantly different from the one in the ground state of the trap (b). It even more drastically differs from the spatial distribution of polaritons in non-condensate fraction, which occupy the excited states in the trap within the $k_B T$ energy range and are delocalized over a region of size $\sim \sqrt{2k_B T/\alpha_{LP}}$. It should be stressed that this difference is due to the envelop function properties of lower polaritons in photonic crystal lattices with small repulsive interactions in polariton system.

For particular trap considered here, the critical threshold number of LPs needed to achieve the BEC phase transition can be estimated from expression $N_c = 1.8(k_B T)^2/(\hbar\omega_{osc})^2$ [16], yielding $N_c = 4.4 \cdot 10^3$ polaritons in the trap at a temperature of 12 K. The non-condensate fraction is delocalized over a region of 40 μm width (about 13 lattice sites), which makes it clearly distinguishable from the condensate fraction at the center cavity pixel of the trap (of $\sim 3 \mu m$ width). The thermal excitation energy $k_B T$ of about 1 meV significantly exceeds the energy separation of quantized LP oscillator states in the trap (21 μeV). Taking also the positive photon-exciton energy detuning into

account, one should expect that such trap favors the thermalization of LPs and spontaneous BEC phase transition in polariton system.

Finally note that the periodic photonic lattice will prevent a localization of exciton polaritons due to disorder effects in the quantum wells, observed in experiments on k-space BEC.

6. CONCLUSION

Photonic crystal heterostructures offer a powerful approach for tailoring the envelope functions of exciton polariton modes propagating in quasiperiodic arrays of microcavities. The use of this concept is illustrated here on example of photonic crystal heterostructure implementing harmonic oscillator trap for exciton polaritons. This concept should stimulate further development of novel applications of polariton-based systems for control of exciton polariton propagation and confinement, and in particular in delivering important evidence that exciton-polaritons might undergo BEC phase transition.

REFERENCES

1. Kasprzak, J., M. Richard, S. Kundermann, A. Baas, P. Jeambrun, J. M. J. Keeling, F. M. Marchetti, M. H. Szymańska, R. André, J. L. Staehli, V. Savona, P. B. Littlewood, B. Deveaud and Le Si Dang, “Bose–Einstein condensation of exciton polaritons,” *Nature*, Vol. 443, 409–414, 2006.
2. Deng, H., D. Press, S. Götzinger, G. S. Solomon, R. Hey, K. H. Ploog, Y. Yamamoto, “Quantum degenerate exciton–polaritons in thermal Equilibrium,” *Phys. Rev. Lett.*, Vol. 97, 146402–4, 2006.
3. Christopoulos, S. G. Baldassarri Höger von Högersthal, A. J. D. Grundy, P. G. Lagoudakis, A.V. Kavokin, J. J. Baumberg, G. Christmann, R. Butté, E. Feltin, J.-F. Carlin, and N. Grandjean “Room–temperature polariton lasing in semiconductor microcavities,” *Phys. Rev. Lett.*, Vol. 98, 126405–4, 2007.
4. Balili, R., V. Hartwell, D. Snoke, L. Pfeiffer, and K. West, “Bose–Einstein condensation of microcavity polaritons in a trap,” *Science*, Vol. 316, 1007–1010, 2007.
5. Deng, H., G. Weihs, C. Santori, J. Bloch, Y. Yamamoto, “Condensation of semiconductor microcavity exciton polaritons,” *Science*, Vol. 298, 199–202, 2002.
6. Weihs, G., H. Deng, R. Huang, M. Sugita, F. Tassone, and Y. Yamamoto, “Exciton-polariton lasing in a microcavity,” *Semicond. Sci. Technol.*, Vol. 18, S386-S394, 2003.
7. Bloch, J., “Polariton quantum degeneracy in GaAs microcavities,” *2008 Latsis Symposium at EPFL on Bose Einstein Condensation in dilute atomic gases and in condensed matter*, 28-30 January 2008, Lausanne (Switzerland), <http://latsis2008.epfl.ch/>.
8. Glauber, R. J., “Nobel Lecture: One hundred years of light quanta,” *Ann. Phys. (Leipzig)*, Vol. 16, 6–24, 2007.
9. Hanbury Brown, R and R. Q. Twiss, “Correlation between photons in two coherent beams of light,” *Nature*, Vol. 177, 27-29, 1956.
10. Glauber, R. J., “The Quantum Theory of Optical Coherence,” *Phys. Rev.* , Vol. 130, 2529–2539, 1963
11. Glauber, R. J., “Coherent and incoherent states of the radiation field,” *Phys. Rev.*, Vol. 131, 2766–2788, 1963.
12. Snoke, D. W., “When should we say we have observed Bose condensation of excitons?,” *Phys. Stat. Sol. (b)*, Vol. 238, 389–396, 2003.
13. Vörös, Z., D. W. Snoke, L. Pfeiffer, and K. West, “Trapping excitons in a two-dimensional in-plane harmonic potential: Experimental evidence for equilibration of indirect excitons,” *Phys. Rev. Lett.*, Vol. 97, 016803–4, 2006.
14. Boiko, D. L., “Paraxial Hamiltonian for photons in two-dimensional photonic crystal microstructures,” *ArXiv* 0710.5287, 1–19, 2007.
15. Boiko, D. L., “Coriolis-Zeeman effect in rotating photonic crystal,” *ArXiv* 0705.1509, 1-12, 2007.
16. V. Negoita et al., “Harmonic-potential traps for indirect excitons in coupled quantum wells,” *Phys. Rev. B*, Vol. 60, 2661–2669, 1999.